Synthesis of a High-Density Phosphonic Acid Functional Mesoporous Adsorbent: Application to Chromium(III) Removal

Kwan H. Nam and Lawrence L. Tavlarides*

Department of Chemical Engineering and Materials Science, Syracuse University, Syracuse, New York 13244

Received October 3, 2004

A high-capacity phosphonic acid functional adsorbent is prepared by co-condensing oligomers of tetraethoxysilane (TEOS) and trimethoxysilylpropyl diethylphosphonate (DEPPS). Hydrolysis/condensation reactions for both silanes are monitored in the sol-state using ^{29}Si NMR spectroscopy, and the dependency of the resulting physicochemical properties on these reaction times is investigated. The molar ratio of TEOS to DEPPS is varied to determine the ratio at which high DEPPS incorporation could be attained without evidence of structural perturbation. The phosphonic acid adsorbent is characterized by solid-state ^{29}Si and ^{31}P NMR spectroscopy, nitrogen sorption, and elemental analysis. The adsorbent exhibits a ligand density of 10.0 mmol P/g, and maximum values of S_{BET} of 437 m^2/g, D_p of 59 Å, and V_p of 0.65 cm^3/g. Further characterization shows an equilibrium chromium(III) adsorption capacity of 82 mg/g at pH 3.6 and rapid adsorption kinetics. Column adsorption at a high space velocity of 156 h^{-1} is achieved with a minimum effluent chromium concentration of 0.01 mg/L. The chromium-loaded adsorbent is stripped using 12 M HCl. A viable synthesis method for the preparation of a high-density functional mesoporous adsorbent is demonstrated.

Introduction

Chromium, classified as a carcinogenic and mutagenic element, is widely used in industries such as metal surface coatings, electroplating, leather tanning, and wood preservatives. Chromium in the generated wastes exists as hexavalent (Cr(VI)) and trivalent forms (Cr(III)), of which the hexavalent form is more toxic. Regardless, Cr(III) removal has received much attention, particularly in leather tanning industries, since a significant fraction of Cr(III) introduced in the process is discarded, thus posing a threat to the environment. Chromium separation from these streams is required for cleanup or reuse. The United States Environmental Protection Agency (USEPA) drinking water maximum contaminant level (MCL) for total chromium is 0.1 mg/L.[1]

The conventional method of treating chromium-bearing streams is chemical precipitation.[2,3] In this process, Cr(VI) is reduced to Cr(III), followed by precipitation of Cr(III) as $Cr(OH)_3$. However, one of the major disadvantages of this method is the production of large amounts of toxic sludge. The use of solid-phase extractants for metal ion adsorption is an alternative method that is considered to be effective in achieving concentrations to low levels. Numerous studies have been conducted on the removal of Cr(III) using various sorbents.[4−9] Among those commonly utilized are polymeric resins and ceramics. Polymeric resins can substantially remove metal ions; however, one of the main disadvantages lies in the swelling of the polymeric skeleton. Ceramic adsorbents, on the other hand, typically have high mechanical strength, chemical, and thermal stabilities, and rigid pore structures. In particular, mesoporous materials are of great interest as they allow molecular accessibility to large internal surface areas and volumes.

The two methods frequently used in preparing adsorptive materials are immobilization of functional groups on bare ceramic surfaces and sol−gel processing. Since the discovery of MCM-41,[10] the ordered mesoporous molecular sieves, various functional groups have been immobilized on pore surfaces of similarly prepared materials for use as adsorbents.[11−16] These materials exhibit high ligand densities and show good adsorption of metal ions from aqueous solutions.

* Corresponding author. Tel.: 1-315-443-1883. Fax: 1-315-443-1243. E-mail: lltavlar@syr.edu.

(1) USEPA. National Primary Drinking Water Standards; Report EPA 816-F-03-016; Washington, DC, 2003.
(2) Yun, Y. S.; Park, D.; Park, J. M.; Volesky, B. *Environ. Sci. Technol.* **2001**, *35*, 4353−4358.
(3) Kratochvil, D.; Pimentel, P.; Volesky, B. *Environ. Sci. Technol.* **1998**, *32*, 2693−2698.
(4) Kocaoba, S.; Akcin, G. *Talanta* **2002**, 23.
(5) Petruzzelli, D.; Passino, R.; Tiravanti, G. *Ind. Eng. Chem. Res.* **1995**, *34*, 2612.
(6) Cordero, T.; Rodriguez-Mirasol, J.; Tancredi, N.; Piriz, J.; Vivo, G.; Rodriguez, J. J. *Ind. Eng. Chem. Res.* **2002**, *41*, 6042.
(7) Yun, Y. S.; Park, D.; Park, J. M.; Volesky, B. *Environ. Sci. Technol.* **2001**, *35*, 4353.
(8) Mendoza, R. N.; Medina, T. I. S.; Vera, A.; Rodriguez, M. A. *Solvent Extr. Ion Exch.* **2000**, *18* (2), 319.
(9) Kabay, N.; Demircioglu, M.; Ekinci, H.; Yuksel, M.; Saglam, M.; Akcay, M.; Streat, M. *Ind. Eng. Chem. Res.* **1998**, *37*, 2541.
(10) Beck, J. S.; Vartuli, J. C.; Roth, W. J.; Leonowicz, M. E.; Kresge, C. T.; Schmitt, K. D.; Chu, C. T−W.; Olson, D. H.; Sheppard, E. W.; McCullen, S. B.; Higgins, J. B.; Schlenker, J. L. *J. Am. Chem. Soc.* **1992**, *114*, 10834.
(11) Walcarius, A.; Etienne, M.; Lebeau, B. *Chem. Mater.* **2003**, *15*, 2161.
(12) Yoshitake, H.; Yokoi, T.; Tasumi, T. *Chem. Mater.* **2002**, *14*, 4603.
(13) Mattigod, S. V.; Feng, X.; Fryxell, G. E.; Liu, J.; Gong, M. *Sep. Sci. Technol.* **1999**, *34*, 2329.
(14) Liu, Y.-H.; Lin, H.-P.; Mou, C.-Y. *Langmuir* **2004**, *20*, 3231.
(15) Antochshuk, V.; Jaroniec, M. *Chem. Mater.* **2000**, *12*, 2496.
(16) Gomez-Salazar, S.; Lee, J. S.; Heydweiller, J. C.; Tavlarides, L. L. *Ind. Eng. Chem. Res.* **2003**, *42*(14), 3404.

10.1021/cm048269v CCC: $30.25
Published on Web 02/17/2005

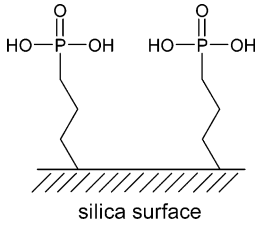

Figure 1. Illustration of phosphonic acid functional SOL-PHONIC adsorbent.

However, upon immobilization of functional groups on these well-defined pore surfaces, loss of surface area and reduction of pore diameter and pore volume can occur. Studies[11,12] have shown that the loss of pore volume can be as high as 60−84%. The degree of pore volume reduction could be a result of the nature of the ligand, such as the size, and the ligand loading. Moreover, a comparative study[17] indicates that materials prepared by the immobilization method appear to have nonuniformly distributed functional groups, whereas the materials prepared by the sol−gel method appear to have uniformly distributed functional groups. In this work, the sol−gel method is employed, which involves the direct co-condensation of organosilanes with cross-linking agents to obtain mesoporous functional adsorbents. Our past studies[16,18−20] have shown that by employing this method, the resulting adsorbents can have high ligand densities and long life cycles. For example, studies on mercury separation[18,19] revealed high adsorption capacities (740 mg/g) from both acidic (2 M HNO_3) and mildly acidic solutions. Less than 10% of the original mercury adsorption capacity is found to be lost after 25 adsorption/desorption cycles of operation,[18] even when concentrated hydrochloric acid is used as the stripping agent for every cycle. Further, the functional groups are shown to be near completely accessible to the metal ions for adsorption.

In this report, the synthesis of a high-density phosphonic acid functional mesporous adsorbent (SOL-PHONIC; Figure 1) by sol−gel processing, and the application to chromium-(III) adsorption from aqueous solutions are presented. Due to our particular interest in adsorptive materials that are applicable to packed-bed operation schemes, the adsorbents are purposely prepared in the form of bulk materials having mesopores and high ligand coverage. The adsorbent is synthesized by co-condensing oligomers of functional precursor silanes (FPS) and cross-linking agents (CA), and by varying the molar ratio of CA to FPS to determine the ratio at which high FPS incorporation can be attained without evidence of structural perturbation. The consequential effects on physicochemical properties are investigated through evaluation of structural properties and chromium equilibrium adsorption. The feasibility of application of the adsorbent to chromium(III) removal from aqueous solutions is examined through batch and column studies.

Table 1. Sol−Gel Processing Parameter Study

	reaction time (h)		
parameter	DEPPS	TEOS	R_{CF}[a]
DEPPS reaction time	0.25	0.25	2
	1	0.25	2
	3	0.25	2
	9	0.25	2
	15	0.25	2
TEOS reaction time	9	0.25	1.25
	9	0.25	1.25
	9	2	1.25
	9	5	1.25
	9	9	1.25
R_{CF}[a]	9	5	2
	9	5	1.5
	9	5	1.25
	9	5	1.125
	9	5	1

[a] R_{CF} = TEOS/DEPPS molar ratio.

Experimental Section

Materials. All reagents used in this study are of analytical reagent (AR) grade obtained from Aldrich, and are used as received. (3-Iodo-propyl)trimethoxysilane [IPTMS; $(CH_3O)_3Si(CH_2)_3I$] is synthesized by refluxing (3-chloropropyl)trimethoxysilane [$(CH_3O)_3Si(CH_2)_3Cl$] with sodium iodide in dry acetone for 48 h. A stock solution of chromium(III) is prepared by dissolving $Cr(NO_2)_3 \cdot 9H_2O$ salt in 2% (v/v) hydrochloric acid.

Functional Precursor Silane Synthesis. The phosphonate functional precursor silane, trimethoxysilylpropyl diethylphosphonate [DEPPS; $(CH_3O)_3Si(CH_2)_3P(O)(OCH_2CH_3)_2$], is synthesized via the Michaelis Arbuzov reaction[21] using IPTMS and triethyl phosphite [TEP; $P(OCH_2CH_3)_3$]. In a typical synthesis, TEP and IPTMS are refluxed in a round-bottomed flask equipped with a condenser for 3 h at 160 °C. Yield = 79%, purity = 99% (GC/MS). Product is purified by vacuum distillation and identified using ^{1}H NMR ($CDCl_3$, 298K): δ 4.03−4.18 (m, 4H), 3.56 (s, 9H), 1.70−1.81 (m, 4H), 1.27 (t, 6H), 0.74−0.79 (m, 2H).

Adsorbent Synthesis. In a solution of DEPPS in ethanol, hydrochloric acid is added while stirring at room temperature. The molar ratio of DEPPS/EtOH/H_2O/HCl is 1:3:3:0.01. The reaction time is varied from 0.25 to 15 h. In another batch of a solution of tetraethoxysilane (TEOS) in ethanol, hydrochloric acid is added while stirring at room temperature. The molar ratio of TEOS/EtOH/H_2O/HCl is 1:4:4:0.005. The reaction time is varied from 0.25 to 9 h. The molar ratio of TEOS/DEPPS, R_{CF}, is varied from 1 to 2.0. Table 1 summarizes the experimental reaction conditions. The two solutions are then mixed to form a homogeneous mixture of the two, followed by the addition of triethylamine [TEA; $N(CH_2CH_3)_3$]. After gel formation, the gel is aged at room temperature for 24 h and dried at 80 °C in an oven for 24 h. The materials are then subjected to reflux in concentrated hydrochloric acid at 80 °C for 24 h to convert the phosphonate groups ($P-OCH_2CH_3$) to phosphonic acids (P−OH).[22] The mixture is cooled to room temperature and the materials are filtered, followed by washing with DI water and acetone. The materials are then dried in an oven at 70 °C overnight. The dried materials are crushed and sieved to desired particle size ranges (75−125 and 125−180 μm) using standard testing sieve ASTME-II specifications (VWR Scientific) sieve trays.

Characterizations. ^{1}H and ^{29}Si NMR and solid-state ^{31}P and ^{29}Si NMR spectra are acquired with a Bruker 600 MHz spectrometer

(17) Lim, M. H.; Stein, A. *Chem. Mater*. **1999**, *11*, 3285.
(18) Lee, J. S.; Gomes-Salazar, S.; Tavlarides, L. L. *React. Funct. Polym*. **2001**, *49*, 159.
(19) Nam, K. H.; Gomes-Salazar, S.; Tavlarides, L. L. *Ind. Eng. Chem. Res*. **2003**, *42*, 1955.
(20) Nam, K. H.; Tavlarides, L. L. *Solvent Extr. Ion Exch*. **2003**, *21* (6), 899.
(21) Arbuzov, B. A. *Pure Appl. Chem*. **1964**, *9*, 307.
(22) Emsley, J.; Hall, D. *The Chemistry of Phosphorus*; John Wiley & Sons: New York, 1976.

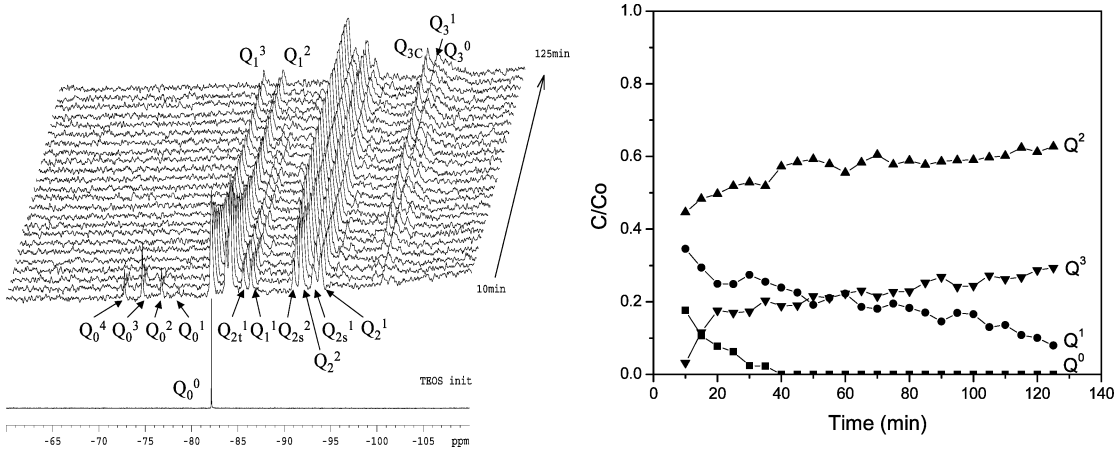

Figure 2. (left) TEOS hydrolysis/condensation reaction monitoring using ^{29}Si NMR spectroscopy. The reaction times are the times at which the measurements of each spectrum are initiated. [Q_i^j, i = number of connected silicon units, j = number of OH groups attached to the silicon atom; s = square cyclic, t = triangular cyclic]. (right) TEOS hydrolysis/condensation reaction cluster speciation [Q^i, i = number of connected silicon units].

following the procedures described elsewhere.[23,24] The number of scans used is 16 for oligomerization reactions conducted at 25 °C. $Cr(acac)_3$ is used as the relaxation agent. Chemical shifts are referenced to tetramethylsilane (TMS) for ^{1}H and ^{29}Si NMR spectra, and H_3PO_4 for ^{31}P NMR spectrum. Elemental analysis is obtained through accredited laboratories: Galbraith Laboratories, Inc., Knoxville, TN and Shiva Technologies, Inc, Syracuse, NY. Nitrogen sorption isotherms are measured on a Micromeritics ASAP 2000 at −196 °C. Samples are outgassed at 150 °C under vacuum for 12 h.

Chromium(III) Adsorption Tests. The pH dependency of chromium adsorption is studied by contacting 0.2 g of adsorbent (75−125 μm particle size range) with 100 mL of 100 mg/L chromium solution at various pH values. Equilibrium adsorption isotherms are measured in batch at pH 2.6, 3.0, and 3.6 by contacting an adsorbent amount of 0.2 g (75−125 μm particle size) with 100 mL of 25−400 mg/L chromium solution in a thermostatically controlled shaker water bath (Precision Scientific model 50) at 25 °C for 24 h. An acetate buffer of 0.05 M is used and the pH is adjusted using hydrochloric acid. In the testing of synthesized materials for chromium adsorption, 200 mg/L chromium solution at pH_e of 3.4−3.6 is used. Chromium concentrations are measured using inductively coupled plasma equipped with a mass spectrometer (ICP-MS ELAN 6100 by Perkin-Elmer). The analytical procedures and methods are conducted according to USEPA standard methods for metal ion analysis. The metal adsorption capacity is calculated by a mass balance difference of the initial and residual solution concentrations.

Kinetic experiments are conducted in a batch reactor using 50, 100, and 200 mg/L chromium solutions at pH 3.5, buffered by 0.05 M acetate. Adsorbents are conditioned in DI water overnight prior to contact with chromium solution to ensure wetting of pores. An adsorbent amount of 0.35 g (75−125 μm particle size range) is introduced to the 250-mL reactor at time zero and samples of the solution are taken at time intervals for analyses of chromium concentrations.

Column adsorption performance is tested by flowing 0.75 L of 200 mg/L chromium solution through a 0.7-cm i.d. column packed with 0.75 g of SOL-PHONIC (125−180 μm particle size range) at a flow rate of 0.45 mL/min (19 BV/h) using a multi-cartridge peristaltic pump. Adsorbents are conditioned in DI water overnight prior to contact with chromium solution to ensure wetting of pores. Glass beads are placed at both ends of the adsorbent bed to ensure even flow of the solution. The effluents from the column are collected for analyses of chromium concentrations. The bed capacity is calculated from the mass balance difference of chromium between the initial and the total effluent solutions. Stripping of the chromium-loaded bed is conducted by flowing 50 mL of concentrated HCl. Washings of the column bed using 10 mL of DI water are performed before and after stripping to ensure discharge of any physically bound or interstitially entrained chromium. Effluent solution is collected for concentration analysis.

Results and Discussion

Synthesis of Phosphonic Acid Functional Adsorbents. The phosphonic acid functional adsorbents are synthesized by co-condensing oligomers of trimethoxysilylpropyl diethylphosphonate (DEPPS) and tetraethoxysilane (TEOS) in an ethanol/hydrochloric acid solution. The oligomerization reactions are monitored using ^{29}Si NMR spectroscopy to determine the desired hydrolysis and condensation reaction times. The first step of the synthesis consists of independently hydrolyzing and condensing DEPPS and TEOS under an acid catalyst (HCl) at room temperature for given periods of time, and the second step consists of adding an organic base to induce gel formation after homogeneous mixing of the two silanes. The independent reaction times of the silanes are determined by monitoring the evolution of oligomeric species with time using ^{29}Si NMR spectroscopy and examining the physicochemical properties corresponding to each of the reaction times. The effect of the molar ratio of TEOS/DEPPS on the resulting material physicochemical properties is also examined.

The evolution of hydrolysis and condensation species of TEOS and DEPPS monitored using ^{29}Si NMR spectroscopy are shown in Figures 2 (left) and 3 (left), respectively. The NMR spectra of the unreacted monomers are also shown at the bottoms of the figures. The chemical shifts of TEOS derivatives, which appear distinctively, concur with those found in the literature.[18,22] Only the clusters of DEPPS condensed species, T^1, T^2, and T^3, appear distinctively, and their ranges of chemical shifts are comparable to those of similar trialkoxysilanes found in the literature.[23,24] It is evident from both spectra that the rates of hydrolysis and condensa-

(23) Sanchez, J.; Rankin, S. E.; McCormick, A. V. *Ind. Eng. Chem. Res.* **1996**, *35*, 117.
(24) Hook, R. J. *J. Non-Cryst. Solids* **1996**, *195*, 1.

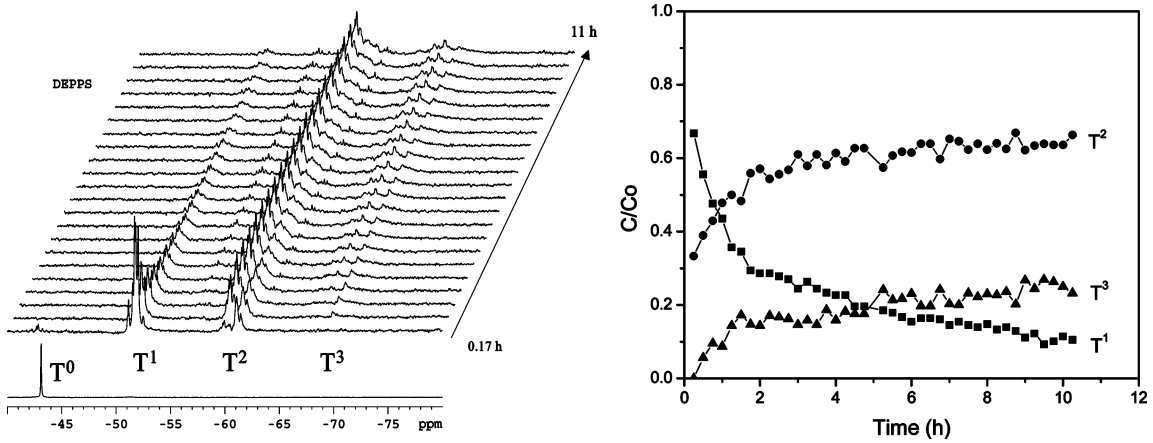

Figure 3. (left) DEPPS hydrolysis/condensation reaction monitoring using ^{29}Si NMR spectroscopy. The reaction times are the times at which the measurements of each spectrum are initiated. [T^i, i = number of connected silicon units]. (right) DEPPS hydrolysis/condensation reaction cluster speciation.

tion of the monomers (T^0) are rapid under the present reaction conditions, in that the hydrolyzed monomers are either low in concentration or completely consumed within 10 min of reaction time. This implies that steric hindrance does not seem to have been a factor in the hydrolysis and condensation reactions of DEPPS despite the bulky phosphonate substituent. This can be explained by the long flexible propyl groups that bridge to the silicon atom, and the presence of methoxy groups (as compared to ethoxy groups for TEOS). The corresponding condensation reaction product analyses for TEOS and DEPPS are shown in Figures 2 (right) and 3 (right), respectively. In the early reaction times, linear species of Q^1 and Q^2, and T^1 and T^2, are dominant, whereas in the long reaction times, a combination of linear and branched species, Q^2 and Q^3, and T^2 and T^3, are dominant. Comparing these results with the corresponding structural properties helps to understand the formation of pore structures. The results are shown in Figure 4 for TEOS and DEPPS. No significant changes in BET surface area, pore diameter, pore volume, and chromium(III) adsorption capacity is observed for TEOS reaction times of 2−9 h; and little difference is observed for reaction times of 0.25 and 2 h. Thus, the initial reaction time of 0.25 h used when analyzing the effect of DEPPS reaction time is appropriate and further study using different reaction times becomes unnecessary. For the DEPPS system, a significant increase in the BET surface area and pore volume with reaction time is evident, whereas the pore diameter remains constant after 1 h. The increase in the chromium(III) adsorption capacity for short DEPPS reaction times is likely to reflect pore channel opening and accessibility to phosphonic acids. The dominant effect of DEPPS reaction time on the physicochemical properties of SOL-PHONIC is attributed to the extent of cavity creation in the vicinity of the phosphonate groups, i.e., with an increase in reaction time, as T^1 species are converted to T^2 and T^3 species producing larger oligomer blocks, the oligomers contain more phosphonate groups that are available for cavity formation. These are then co-condensed with TEOS clusters in building up the gel framework. On the basis of these results, the reaction times used for further investigation are 5 h for TEOS and 9 h for DEPPS (reaction times when T^1 and Q^1 are minimal in concentrations).

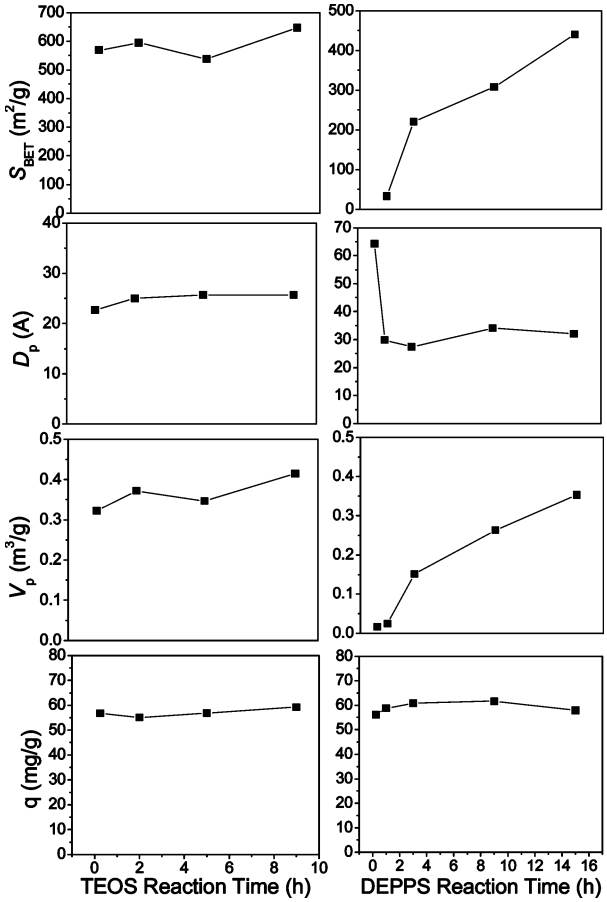

Figure 4. Effect of TEOS and DEPPS reaction times on physicochemical properties of SOL-PHONIC.

The gel times recorded for both the TEOS and the DEPPS indicate that with increases in the hydrolysis and condensation reaction times, gel times decreased. Gel times in most cases are recorded as <30 min, with opaque gel appearances. This trend in the gel times is likely due to the lower cross-linking that is required to form a gel, as large oligomeric blocks are already formed during independent hydrolysis and condensation reactions. Thus, the hydrolysis/condensation reaction times of the FPS affect the physicochemical properties and gel times, whereas the reaction times of the CA primarily affect the gel times. These parameters, by which oligomer formation is controlled, therefore become important when preparing porous functional materials.

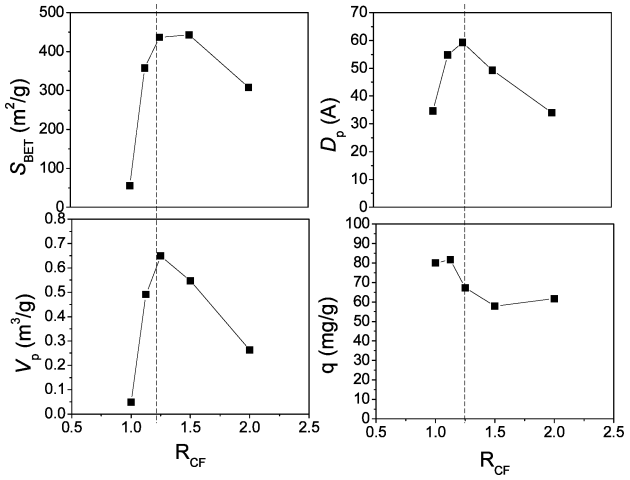

Figure 5. Effect of R_{CF} on physicochemical properties of SOL-PHONIC.

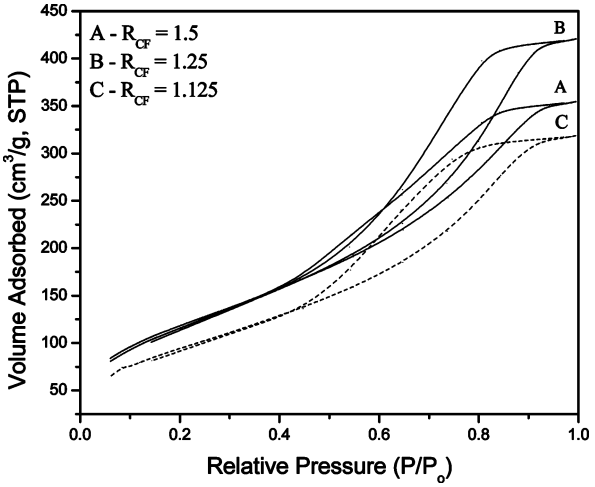

Figure 6. Nitrogen adsorption−desorption isotherms of SOL-PHONIC.

The molar ratio of TEOS to DEPPS, R_{CF}, is the measure of the functional group content in the solid adsorbent, which determines the theoretical metal ion adsorption capacity. Figure 5 shows the variation in physicochemical properties with various molar ratios. It is observed that the optimal values of BET surface area, pore diameter, and pore volume occur when $R_{CF} = 1.25$, which theoretically represents 44 mol % of DEPPS in the material. The decrease in these characteristic values with an increase in DEPPS content beyond the optimal point likely implies that the physical configuration of the structure is weakened by insufficient cross linking that occurs as less tetra functional silicon alkoxide (TEOS) exists. This circumstance can promote the collapse of pore channels during drying. Thus, a decrease in pore size or even blockage of pore openings may occur, which then prevents molecular accessibility to phosphonic acids. On the other hand, chromium adsorption capacity continues to increase even after the pore sizes start decreasing until it reaches a maximum value at $R_{CF} = 1.125$, and the capacity drops thereafter. This occurrence in the decrease in capacity can be attributed to the fractions of ligands that begin to become inaccessible to chromium ions upon pore structure changes. Regardless, a capacity of 82 mg/g is observed when $R_{CF} = 1.125$.

The nitrogen adsorption−desorption isotherms for three SOL-PHONIC samples having R_{CF} values of 1.5, 1.25, and 1.125 are shown in Figure 6. They all exhibit type IV isotherms, characteristic of mesoporous materials, and capillary condensation steps at a relative pressure of 0.4. As DEPPS content increases (from $R_{CF} = 1.5$ to 1.125), the pore volume and average pore diameter increase from 0.55 to 0.65 cm^3/g and 49 to 59 Å (isotherms A and B), respectively, whereas the surface area does not change significantly, i.e., 443 to 437 m^2/g. The increases in the pore volume and average pore diameter are attributed to the higher fraction of mesoporous channels formed by phosphonates. However, with a further increase in the incorporation of phosphonate groups, a significant difference from the other isotherms is shown in that the isotherm C departs from the main shapes, leading to lower pore volume, pore diameter, and surface area, and exhibits a wider hysteresis loop. This phenomenon implies that a physical limitation is reached as the framework is weakened, as discussed in the previous section.

Adsorbent Characterization. The ligand density of SOL-PHONIC resulting from using R_{CF} of 1.25 in the synthesis mixture is determined by elemental analysis employing accredited laboratories. Results from Galbraith Laboratories, Inc. and Shiva Technologies, Inc. indicate values of 9.7 ± 0.8 and 10.4 ± 0.3 mmol P/g, respectively. The average value of these two ligand densities is 10.0 mmol P/g. This high ligand density is a result of using a large fraction of DEPPS in the synthesis mixture.

Information on the extent of incorporation of DEPPS and the silicon environment of the adsorbent material is provided by solid-state ^{29}Si NMR analysis. The ^{29}Si CP-MAS and ^{29}Si MAS NMR spectra are shown in Figure 7. The strong resonance of T^2 and the weak resonance of T^1 shown in Figure 7a illustrate that DEPPS is predominantly cross-linked by two other silicon units. Another ^{29}Si CP-MAS spectra acquired on the same material one year later shows no difference, implying that the adsorbent is stable at room temperatures. Quantitative analysis of peak areas of the spectra shown in Figure 7b shows that the Q/T ratio is 1.3, indicating that the material is comprised of 43% DEPPS. This value implies that DEPPS is highly incorporated in the material. The results also demonstrate that the material is composed primarily of only two species, T^2 and Q^3, which is estimated to represent 82% of the material. The prominent presence of these two species suggests that a high population of hydroxyl groups exist that can provide hydrophilic characteristics for effective applicability to aqueous systems. Chemical stability of the material is expected, however, even in the dominant presence of T^2 and Q^3 species. A previously synthesized adsorbent bearing thiol groups also exhibiting similar ^{29}Si MAS NMR spectra, in that T^1, T^2, Q^2, and Q^3 species are present and T^3 and Q^4 species are not observed, shows excellent multi-cycle operation. Specifically, the adsorption capacity loss after 25 cycles of adsorption/desorption is found to be <10% even when employing 12 M HCl solution as the stripping agent for every cycle.[19]

Figure 8 shows the ^{31}P CP-MAS NMR spectrum of SOL-PHONIC. A single peak is observed at $\delta = 32.1$ ppm, reflecting complete hydrolysis of the phosphonates to phosphonic acids and thus the presence of phosphonic acid groups only. The chemical shift agrees with that found in the

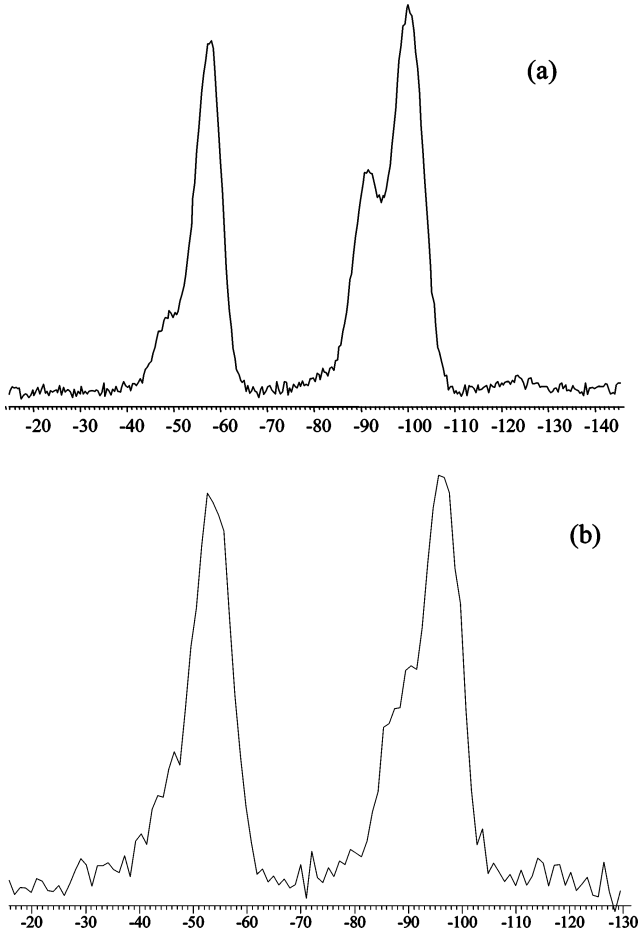

Figure 7. (a) ^{29}Si CP-MAS NMR of SOL-PHONIC. (b) ^{29}Si MAS NMR of SOL-PHONIC. Q/T = 1.3; δ = (T^1, −49.1; T^2, −58.1; Q^2, −91.6; Q^3, −100.2) ppm.

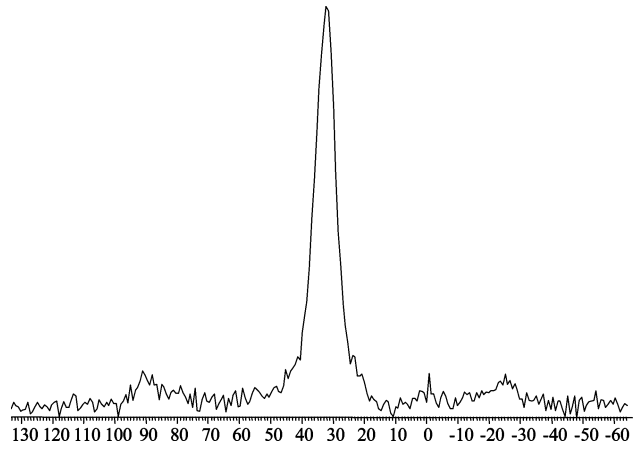

Figure 8. ^{31}P CP-MAS NMR of SOL-PHONIC, δ = 32.1 ppm.

literature.[25] This result implies that the ligand density of 10 mmol P/g is an implication of 10 mmol of phosphonic acid groups per gram of adsorbent.

Chromium(III) Adsorption Tests. The phosphonate groups of SOL-PHONIC are hydrolyzed to phosphonic acids under 12 M HCl solutions for 24 h prior to chromium adsorption tests. Although this treatment is employed to activate the metal binding sites, it also demonstrates the chemical and thermal stability of the ligands in harsh acidic

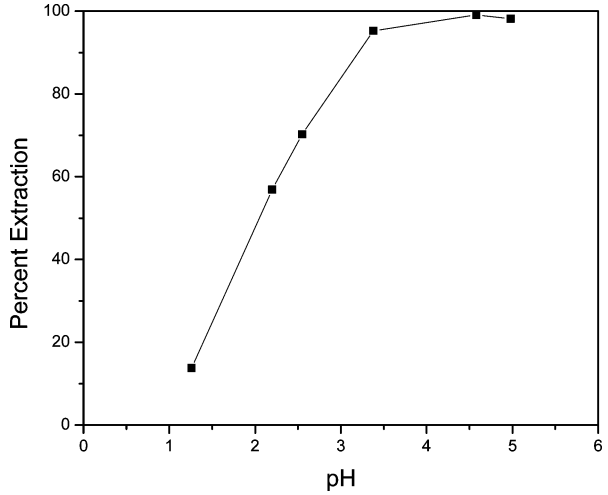

Figure 9. pH Isotherms of chromium; $[Cr]_o$ = 100 mg/L, volume = 100 mL, weight = 0.2 g, contact time = 24 h, buffered by 0.05 M acetate.

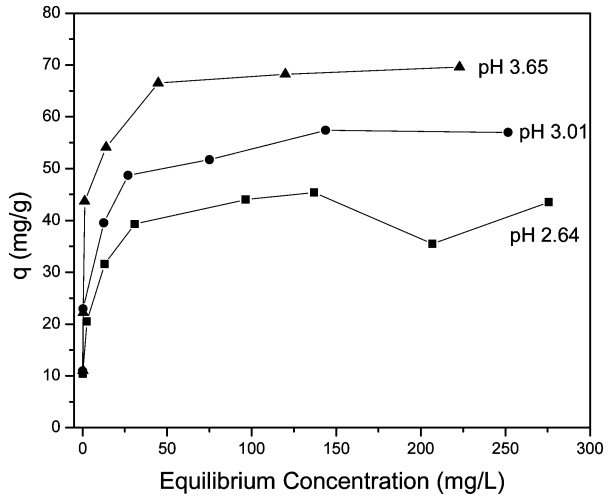

Figure 10. Adsorption isotherms of chromium at three different pH values; volume = 100 mL, weight = 0.2 g, contact time = 24 h, buffered by 0.05 M acetate.

conditions. Metal ion adsorption tests before hydrolysis (using phosphonates) revealed no adsorption activity, which also implies negligible adsorption on the silica surface. Activity loss due to condensation of P−OH groups to form P−O−P linkages is not expected since P−O−P linkages are hydrolyzed to acids in the presence of water.[26]

The effect of pH on chromium adsorption is evaluated from pH 1 to 5 as shown in Figure 9. The percent of chromium extraction increases with an increase in pH in the range studied, where the maximum is found at pH 4.5. During preliminary experiments, a drop in pH is observed after equilibrium is reached, which implies that protons are released upon chromium adsorption. This observation suggests that the H+ displacement mechanism has occurred. The equilibrium adsorption isotherms for the three different equilibrium pH values (2.64, 3.01, and 3.65) are shown in Figure 10, and the corresponding maximum adsorption capacities are summarized in Table 2. These pH values are selected for this study because the pHs of leather tanning wastewaters lie in the range of 2.5−4.[5] At pH 3.65, the

(25) Corriu, R. J. P.; Datas, L.; Guari, Y.; Mehdi, A.; Reye, C.; Thieuleux, C. *Chem. Commun*. **2001**, 763.

(26) Thomas, L. C. *The Identification of Functional Groups in Organophosphorus Compounds*; Academic Press: New York, 1974.

Table 2. Chromium(III) Adsorption Isotherm Results

pH_e	q_{max} (mg/g)
2.64 ± 0.06	43.5
3.01 ± 0.08	57.0
3.65 ± 0.14	69.6

maximum chromium adsorption capacity is found to be close to 70 mg/g (1.35 mmol/g); however, somewhat higher adsorption capacities are expected at higher pH values, as the pH isotherm indicates. Speciation calculations using MINEQL+[27] show that the $Cr(H_2O)_6^{3+}$ and $Cr(OH)(H_2O)_5^{2+}$ species (fully hydrated forms) exist in the pH range of 2−5. Both of these chromium species are expected to participate in the adsorption mechanism through cationic-exchange processes.[8,28] If so, the expected maximum adsorption capacities would be 3.33 mmol/g if only the trivalent species is adsorbed, 5 mmol/g if only the divalent species is adsorbed, and between these two values if both were to participate in the adsorption mechanism. However, since the observed adsorption capacity at pH 3.65 is 1.35 mmol/g, either many binding sites are not occupied or steric hindrance is the reason behind the lower than expected value due to the requirement of two or three sites for adsorption to take place.

The kinetic data of SOL-PHONIC are presented in Figure 11. For the three chromium concentrations examined, near

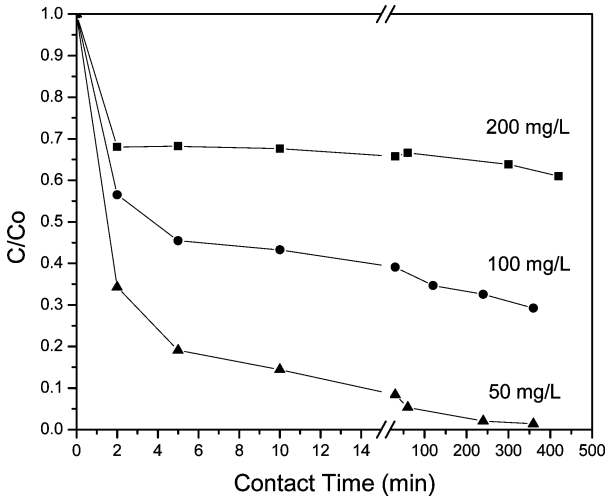

Figure 11. Adsorption kinetics of chromium using 50, 100, and 200 mg/L solutions at pH 3.6; volume = 250 mL, weight = 0.35 g, particle size = 75−125 μm.

equilibria are reached rapidly within minutes of contact time, reflecting the presence of minimal mass transfer resistances. The gradually decreasing trends in concentrations observed in the long contact times for all three cases may be due to the steric hindrance from the preoccupied surface sites in accommodating additional chromium ions and to the diminished availability of the required number of sites being closely spaced.

Dynamic adsorption is studied in fixed-bed operational schemes for two column bed sizes using two different flow

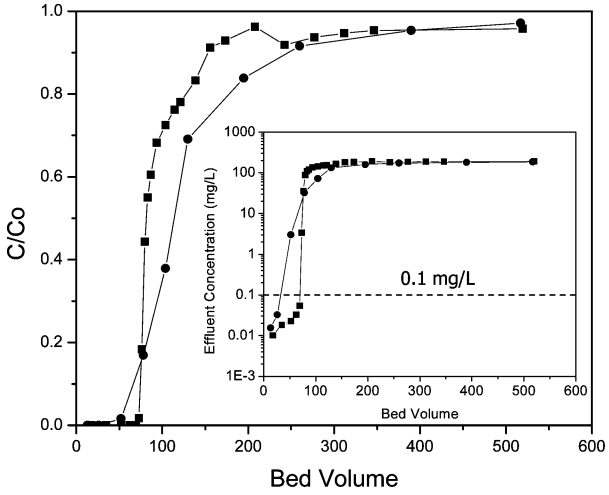

Figure 12. Breakthrough curve of chromium using 200 mg/L solution at pH 3.6: (●) volume = 200 mL, weight = 0.2 g, Q = 1 mL/min (156 h^{-1}), bed volume (BV) = 0.385 cm^3; (■) volume = 750 mL, weight = 0.75 g, Q = 0.45 mL/min (19 h^{-1}), BV = 1.44 cm^3. Inset: effluent concentration against bed volume showing EPA MCL of 0.1 mg/L for total chromium.

rates. A comparison of the two breakthrough curves is shown in Figure 12. Despite the differences in flow rates, sharp breakthrough curves are evident in both cases. However, toward saturation, long tails in the curves are observed (although this is less pronounced in the slower flow rate system). These phenomena are likely due to the requirement of multiple ligands per chromium ion for adsorption to take place. Moreover, for both columns, the effluent concentrations (<0.02 mg/L) are far below the maximum contaminant level of 0.1 mg/L regulated by the USEPA for total chromium. This reflects substantial extraction efficiency of the SOL-PHONIC adsorbent, even with the very high flow rate of 156 h^{-1}. Regeneration, tested on the short bed, is found feasible with 12 M HCl with a stripping efficiency of >90%.

Chromium(III) adsorption using SOL-PHONIC is quantitatively compared with other materials, as shown in Table 3, by means of adsorption capacities and structural properties. Among the materials shown in the table that vary in functional groups and material supports, Amberlite XAD-2 and Diphonix resins have functional groups that are similar to SOL-PHONIC. The former material exhibits attractive structural features, however it shows very low adsorption capacities. The latter material, originally developed for the separation of actinides,[29] exhibits chromium adsorption properties; however, the capacity is observed to be less than that of SOL-PHONIC. The SOL-PHONIC adsorbent developed in this work, exhibiting an adsorption capacity of 82 mg/g (when R_{CF} of 1.125 is used in the synthesis) and rapid kinetics, shows promise for chromium adsorption.

Conclusions

This work demonstrates that a mesoporous adsorbent bearing high density of phosphonic acid groups can be synthesized by co-condensing oligomers of FPS and CA. The

(27) Schecher, W. D.; McAvoy, D. C. MINEQL+ A Chemical Equilibrium Modeling System, Version 4.0; Environmental Research Software: Hallowell, Maine, 1998.
(28) Gumienna-Kontecka, E.; Jezierska, J.; Lecouvey, M.; Leroux, Y.; Kozlowski, H. *J. Inorg. Biochem.* **2002**, *89*, 13.
(29) Chiarizia, R.; Horwitz, E. P.; D'Arcy, K. A.; Alexandratos, S. D.; Trochimczuk, A. W. *Solvent Extr. Ion Exch.* **1996**, *14* (6), 1077−1100.

Table 3. Comparison of Materials for Chromium(III) Adsorption

material	q mg/g	D_p A	V_p m^3/g	S_{BET} m^2/g	material support	functional ligand	reference
SOL-PHONIC	82	44	0.43	397	silica	phosphonic acid	this work
activated carbon	32		0.34	730	carbon	oxidized carbon	6
seaweed biomass	34				biomass	seaweed biomass	2
Amberlite	6.5	90[a]	0.65[a]	300[a]	resin	Cyanex 272 (phosphinic acid)	8
Diphonix	50[b]				resin	diphosphonic acid	9
Purolite C106	55		macroporous		resin	carboxylic acid	5

[a] Data from www.sigmaadrich.com. [b] Estimated from breakthrough curve.

ligand density can be maximized by varying the TEOS to DEPPS (R_{CF}) molar ratio. The role of the FPS and CA oligomers in the sol−gel synthesis is further understood by relating the sol-state synthesis compositions to the resulting solid-state properties. The adsorbent structural properties are found to be primarily dependent on the oligomeric species of the FPS rather than those of the CA. By maximizing the FPS incorporation through varying the molar ratio of the FPS and CA, the adsorbent is found to exhibit a high ligand density of 10 mmol P/g.

Application of the adsorbent to chromium(III) adsorption is demonstrated. Results show an equilibrium adsorption capacity higher than that of other materials found in the literature. Kinetics results show that near equilibrium is reached in as little as 2 min of contact time. Column tests show dynamic operation at high throughput with sharp breakthrough curves and effluent concentrations far below the USEPA MCL level of total chromium.

Acknowledgment. The financial support of the National Science Foundation through Grant CTS-0120204 is gratefully acknowledged. We thank Mr. David Kiemle at the State University of New York, Environmental Science and Forestry, for assistance with NMR spectroscopy.

CM048269V